

Covert optical detection under adverse weather conditions (2022-2023)

Ilkka Tittonen, Matti Raasakka, Arttu Pönni, Vladimir Kornienko

Micro and Quantum Systems (MQS) group
Department of Electronics and Nanoengineering
Aalto University

ilkka.tittonen@aalto.fi

16 November 2023

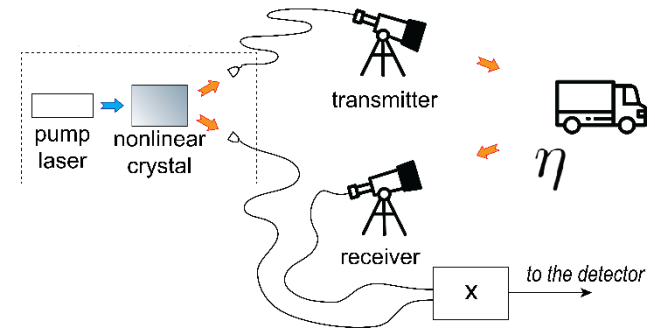
Outline:

- ❑ Introduction and project description
- ❑ Target detection with correlated photons
- ❑ Light source optimization
- ❑ System performance
- ❑ Potential applications
- ❑ Summary and Outlook

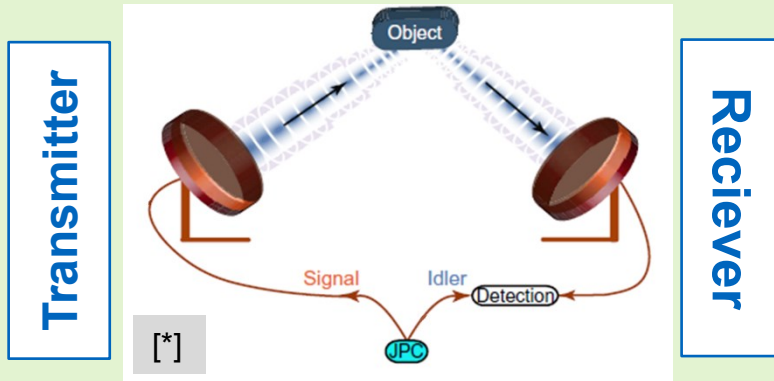
Introduction: correlation-enhanced target detection

An entanglement-based approach to improving an optical radar's capability to detect a weakly-reflecting target embedded in background noise that can be much stronger than the target return.

[J.H. Shapiro // *IEEE A&E Systems Magazine* 35, 8-20 (2020).]

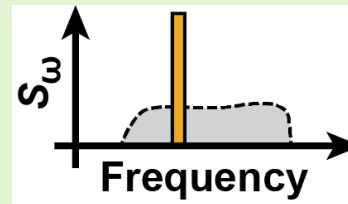


Boosting the performance of a radar

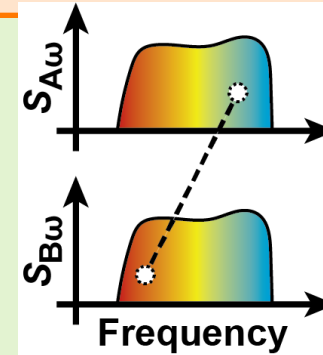


Can the entanglement* survive an entanglement-breaking lossy channel?

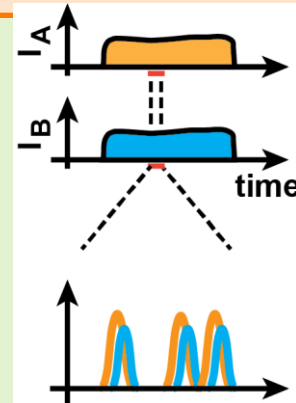
$$* |\Psi_{AB}\rangle \neq |\Psi_A\rangle |\Psi_B\rangle$$



classical



VS
quantum



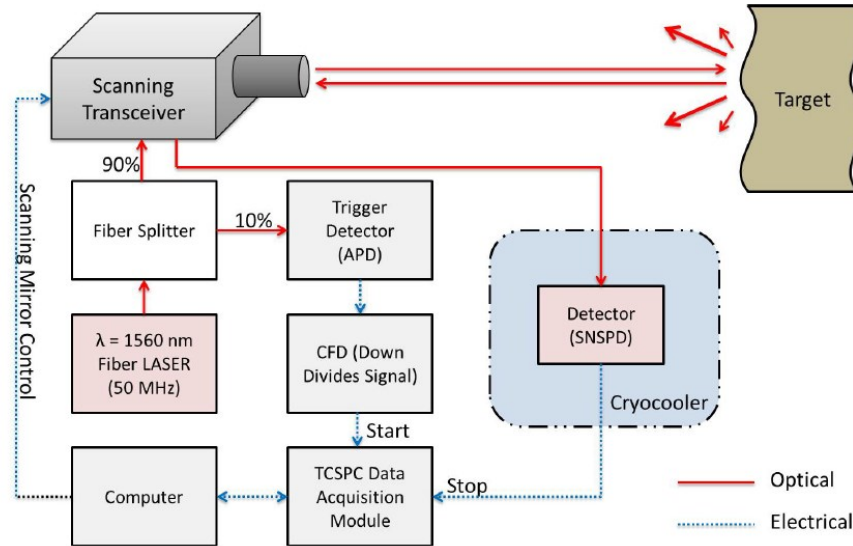
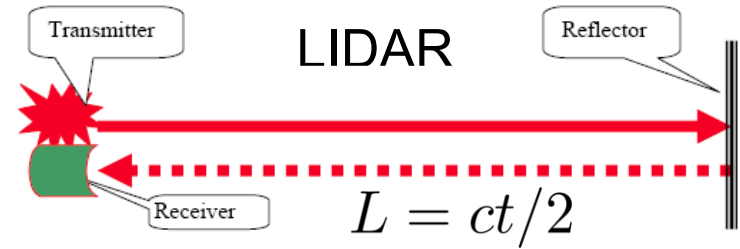
- Initial suggestion: Signal-to-noise improvement of 2^d times (d – number of modes)
- Signal-to-noise improvement of +6 dB over any conceivable classical radar
- Noise rejection, large number of modes needed.

Broad spectrum, large time interval, random values for each realization => makes hard to observe externally

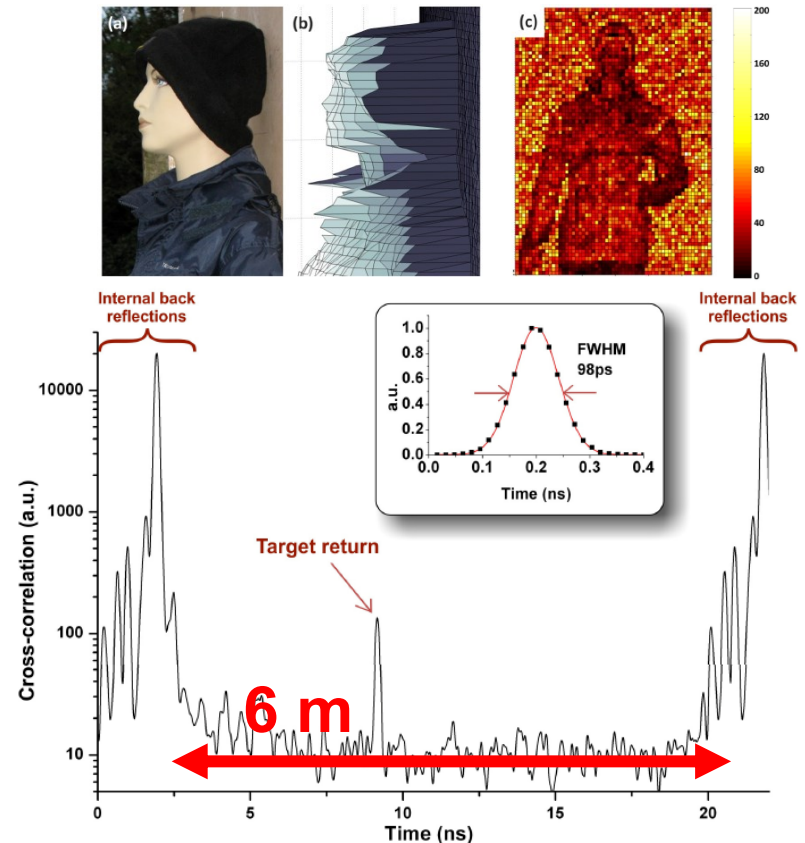
Optics: Existing methods for target detection

Lidar (**L**ight **D**etection and **R**anging) approach:

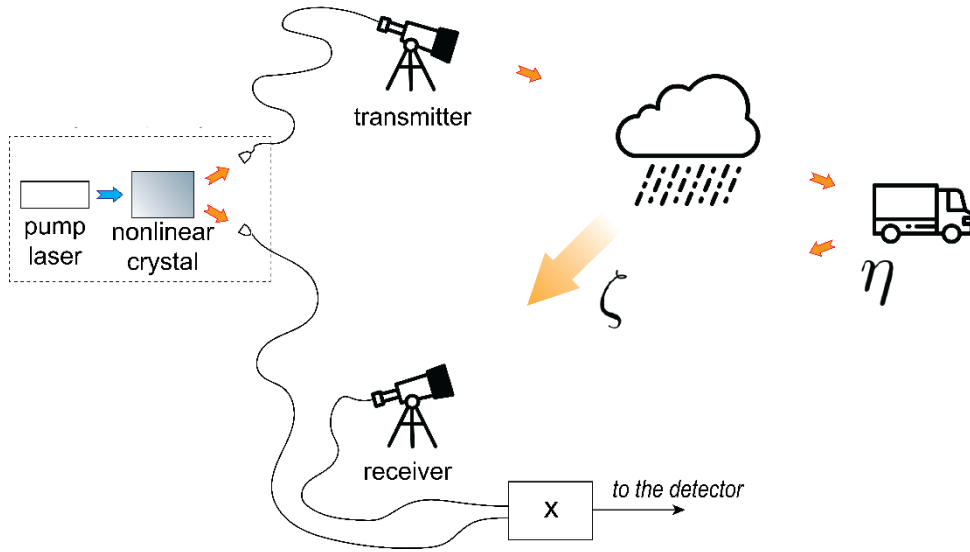
- send a pulse;
- detect reflection;
- measure the elapsed time.



- Operating distance: $\sim 1 \text{ km}$ (*)
- Depth imaging: $\sim 1 \text{ mm}$ resolution (*)
- Optical output: $1.5 \mu\text{m}$, 50 MHz, $< 1 \text{ ps}$, 250 μW mean = 5 W peak
- Detection: cryogenically cooled (3 K) superconducting nanowire



Drawbacks of conventional detection under adverse weather conditions



Rain, fog, and snow introduce additional scattering. More losses to the signal, greater visibility of the source to external observers.



Radiofrequency range: strong background from the atmosphere.



Covert surveillance: scattering of the transmitted radiation makes the illumination source visible to an external observer.



Microscopy applications: reflection from the cover glass; scattering from the tissues.

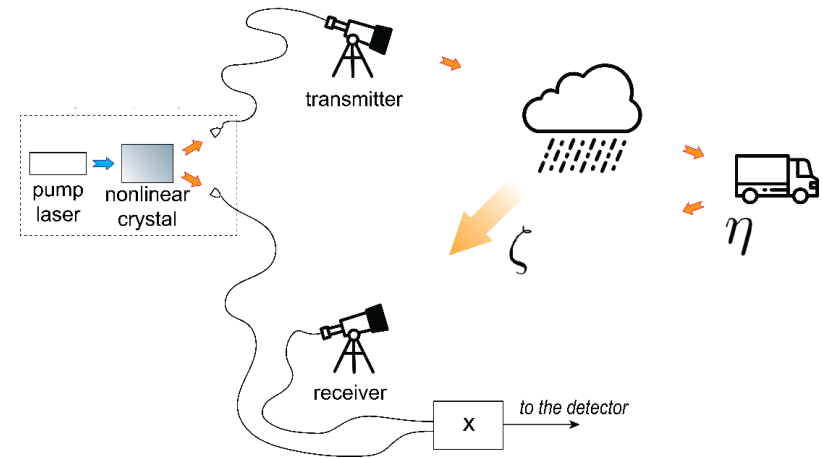
Covert optical detection under adverse weather conditions

Project goal:

to study the impact of heterogeneous dynamically changing environment on the performance of a correlation-based target detection system.

Proposed methods:

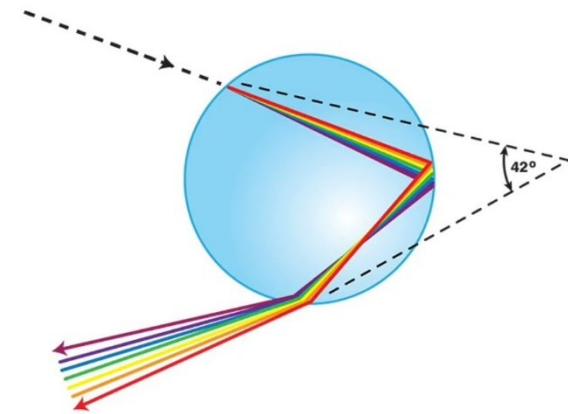
- ❑ correlated beams for increasing the signal-to-noise ratio and keeping the values of instantaneous and mean power at low level;
- ❑ change the type of the optical source;
- ❑ novel data processing techniques.



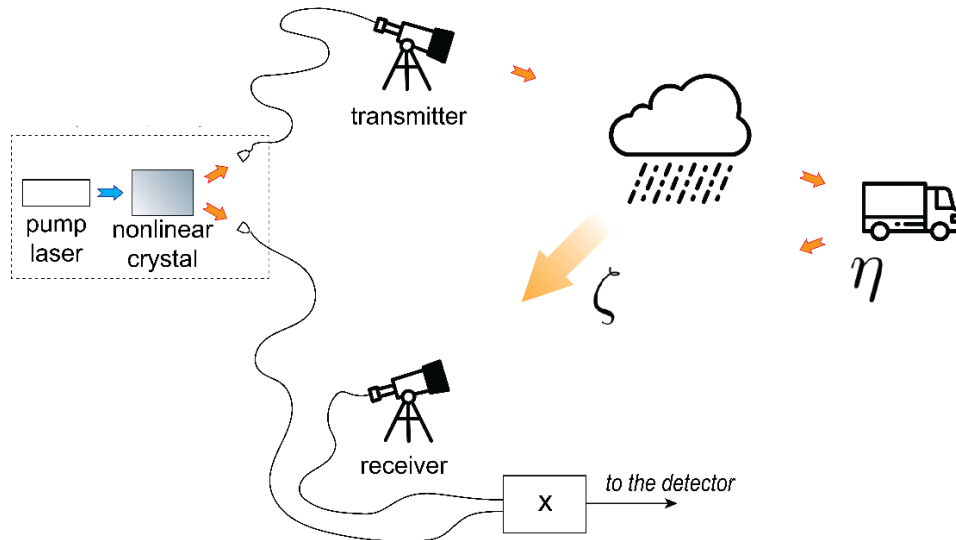
Research objectives:

1. to design a broadband source of correlated beams based on a nonlinear-optical crystal;
2. to elaborate data processing techniques to maximize the detection efficiency;
3. to estimate the achievable properties of the system in terms of operating distance, speed, and the detection efficiency as a function of the emitted optical power.

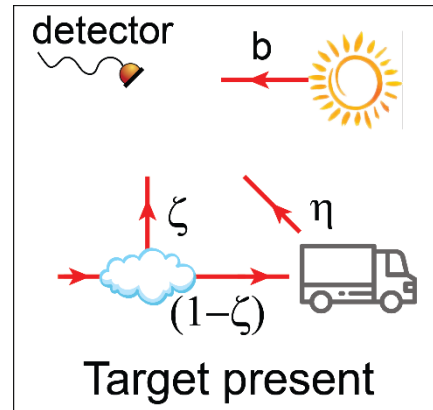
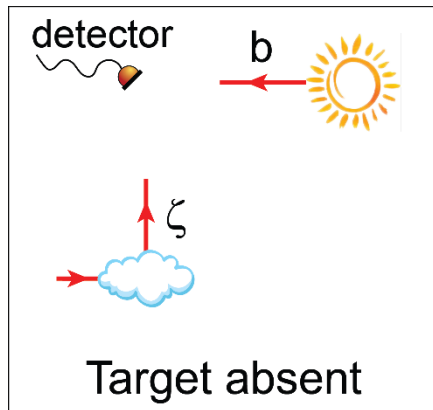
How to model rain droplets / fog?



- ❑ Main effect: additional reflectance (ζ)
- ❑ Losses are taken into account by reducing the target effective reflectance (η)



How to model rain droplets / fog?



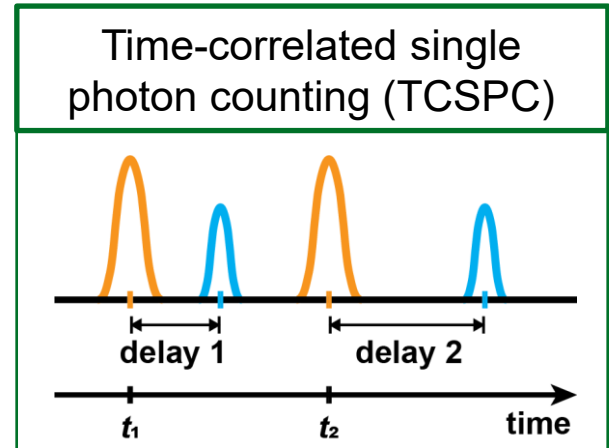
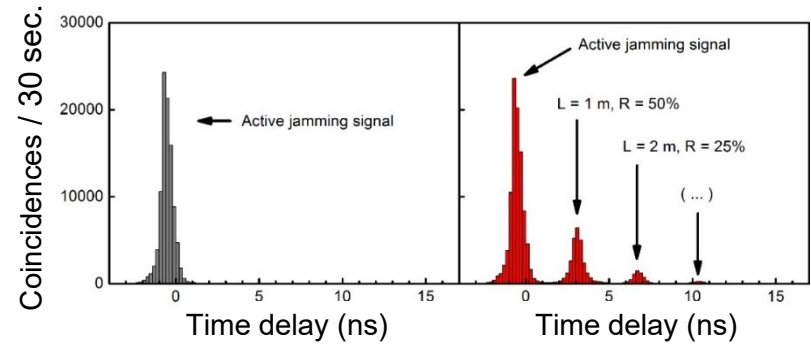
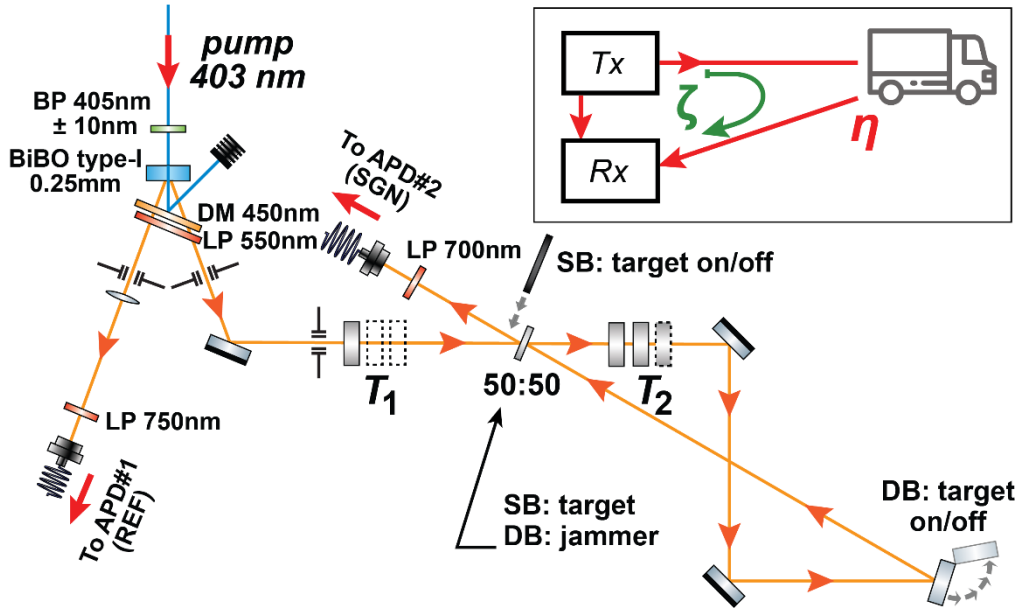
(idler beam not shown)

- ❑ Background noise is not correlated with the stored idler beam.
- ❑ A jamming object (“jammer”) passively reflects part of the radiation sent to the target. Perfect correlations!
- ❑ The more one sends, the greater the noise.

- ❑ Main effect: additional reflectance (ζ) **“jamming object”**
- ❑ Losses are taken into account by reducing the target effective reflectance (η)

Research question: how to minimize the impact of the jamming object on the correlation-enhanced target detection with entangled photons.

Target detection with correlated photons



Partially Reflecting Jamming Objects in Correlation-Enhanced Target Detection
 V.V. Kornienko,¹ C. Vidal,^{1,2} A. Pönni,¹ M. Raasakka,¹ and I. Tittoonen,¹
¹Department of Electronics and Nanoengineering, Aalto University, FI-00076 Espoo, Finland
²Blackett Laboratory, South Kensington Campus, Imperial College London SW7 2BZ London, United Kingdom
 (*Electronic mail: vladimir.kornienko@aalto.fi.)
 (dated: 4 October 2022)

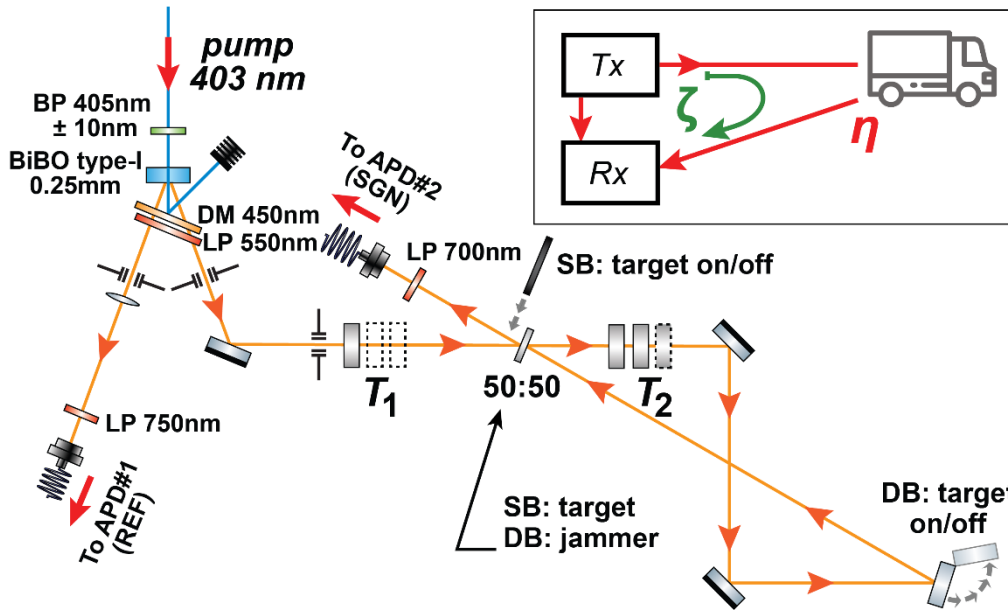
In optical detection of distant objects one can benefit from quantum correlations-enhanced protocols. We demonstrate that when no distinction can be made between the jammer and the target, the performance of the detection protocol can be improved by using quantum correlations. We derive the performance of the detection protocol and show that it can be improved by using quantum correlations. We demonstrate that when no distinction can be made between the jammer and the target, the performance of the detection protocol can be improved by using quantum correlations.

Mist generator OFF

Mist generator ON

- Single-beam interrogation (SB): only APD#2 is used; APD#1 (REF) is ignored.
- Double-beam interrogation (DB): both APD#1 and APD#2 are used; coincidence detection.

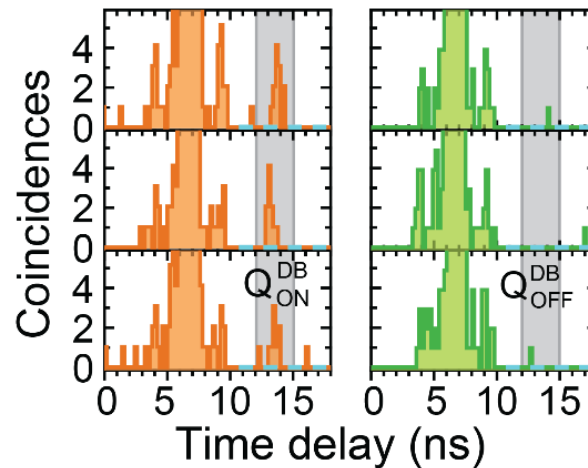
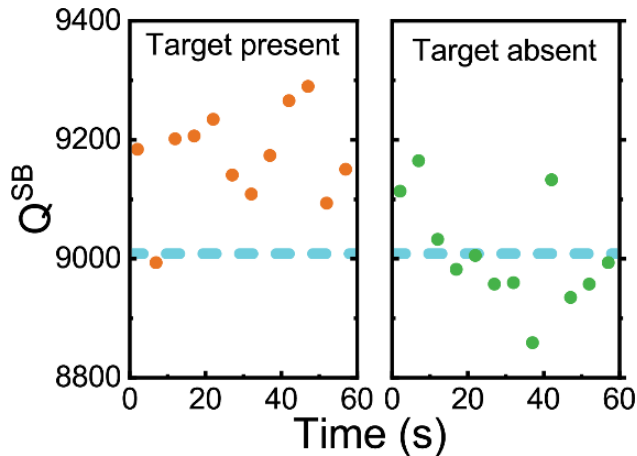
Target detection with correlated photons



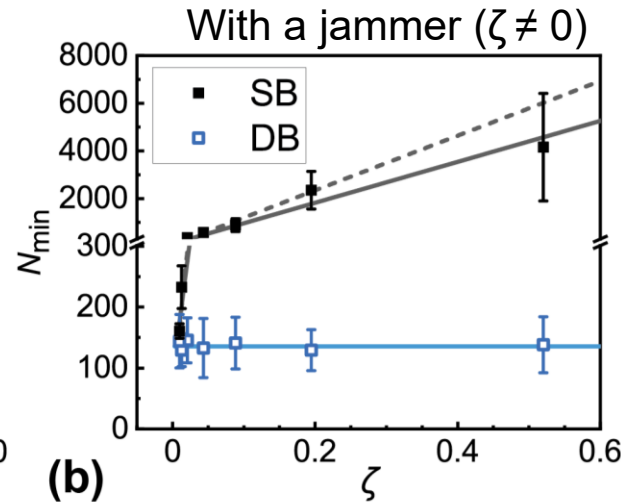
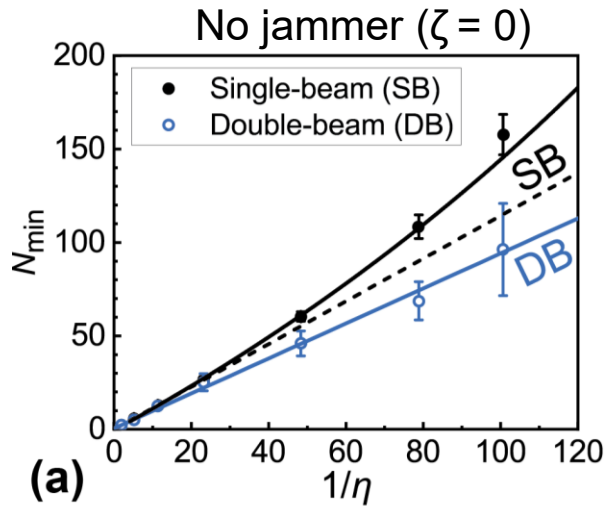
- Single-beam interrogation (SB): only APD#2 is used; APD#1 (REF) is ignored.
- Double-beam interrogation (DB): both APD#1 and APD#2 are used; coincidence detection.

Radiation coming from the jammer (ρ'_J) and from the target (ρ'_T) can be described by an indistinguishability parameter μ :

$$\mu \equiv \frac{\text{Tr } \rho'_J \rho'_T}{\text{Tr } \rho'^2_T}, \quad \mu \in [0; 1]$$



Target detection with correlated photons



$$N_{min}^{SB} \propto \frac{\eta + \mu^{SB}\zeta + b}{\eta^2}$$

($\mu^{SB} = 1$: fully indistinguishable)

$$N_{min}^{DB} \propto \frac{\eta + \mu^{DB}\zeta + b/d}{\eta^2}$$

($\mu^{DB} = 0$: fully distinguishable)

b – number of background photons per mode; d – number of modes.

- We derived the equations governing the performance of the target detection protocol under jamming.
- The impact of the jammer can be described with a parameter μ .
- A jamming object with the reflectance ζ deteriorates the performance of the target detection protocol by a factor of $\zeta / b d$.
- We performed correlation-enhanced target detection with optical entangled photon pairs at 800 nm.
- The results can be applied to the design of target detection protocols and in developing advanced imaging techniques.

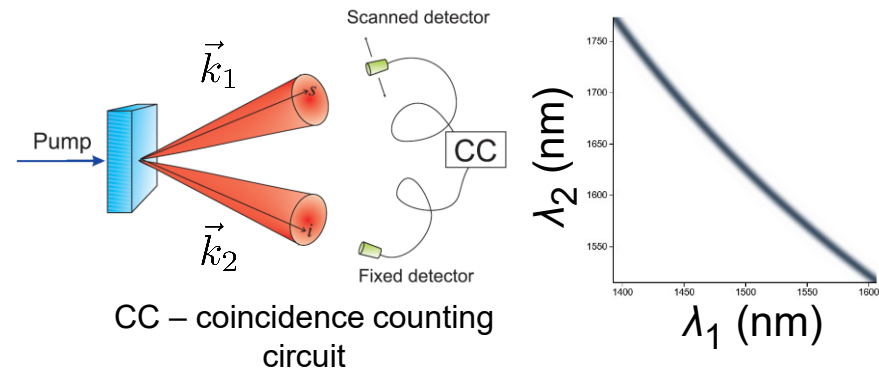
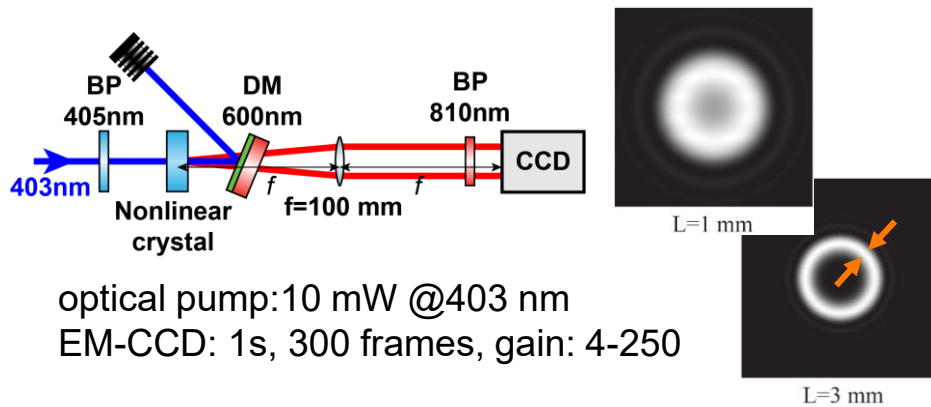
Source optimization

Unconditional photon detection probability (single counts):

$$\frac{dw^{uncond}}{dk_{1\perp x}} = \int dk_{2\perp x} |\Psi(k_{1\perp x}, k_{2\perp x})|^2$$

Conditional photon detection probability (coincidences):

$$\frac{dw^{cond}}{dx_1} = \frac{|\Psi(k_{1\perp x}, k_{2\perp x})|^2}{\int dk_{1\perp x} |\Psi(k_{1\perp x}, k_{2\perp x})|^2} \Big|_{k_{2\perp x}}$$



$\Psi(\mathbf{k}_1, \mathbf{k}_2)$ is a biphoton field amplitude.

It can be computed using the formalism of macroscopic nonlinear optics.

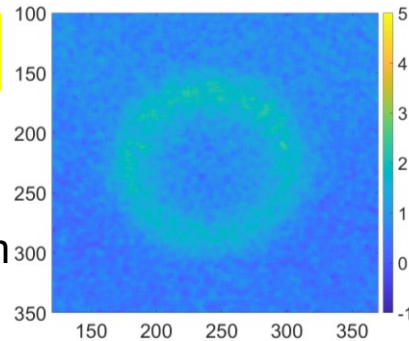
- ❑ Optimization goal: maximize w^{cond} in the region of interest.
- ❑ Photon source already saturates the detection system => keep the value of w^{cond} constant while making the source more broadband.

Source optimization

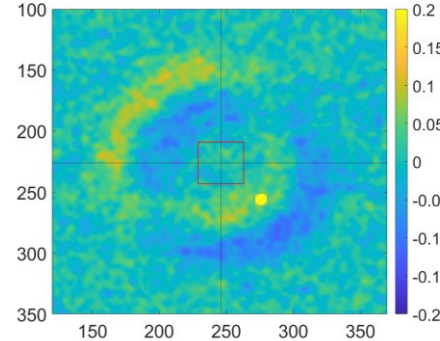
Broadband source:
time per frame: **2 sec.**

BiBO (bismuth borate)
length 0.25 mm
pump beam waist 0.1 mm
pump bandwidth 5 nm

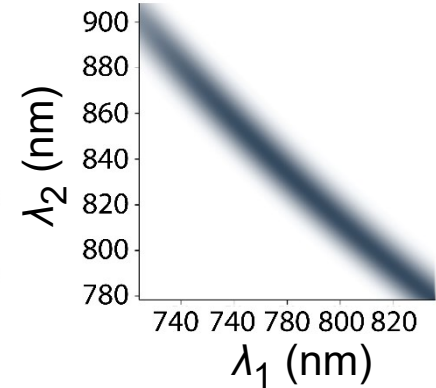
Unconditional probability (w^{uncond}):



Correlation coefficient:

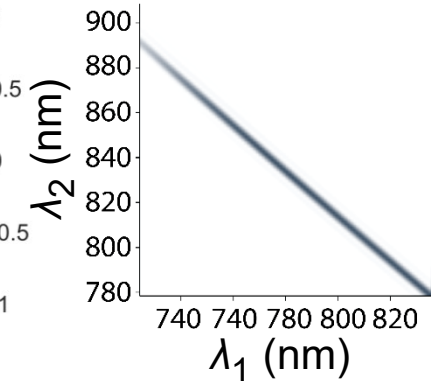
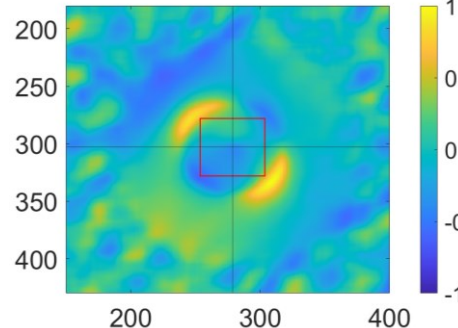
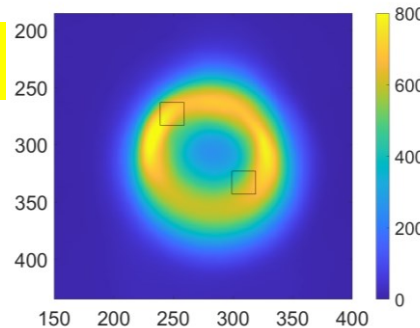


Conditional probability (w^{cond}):



High-flux source:
time per frame: **15 ms**

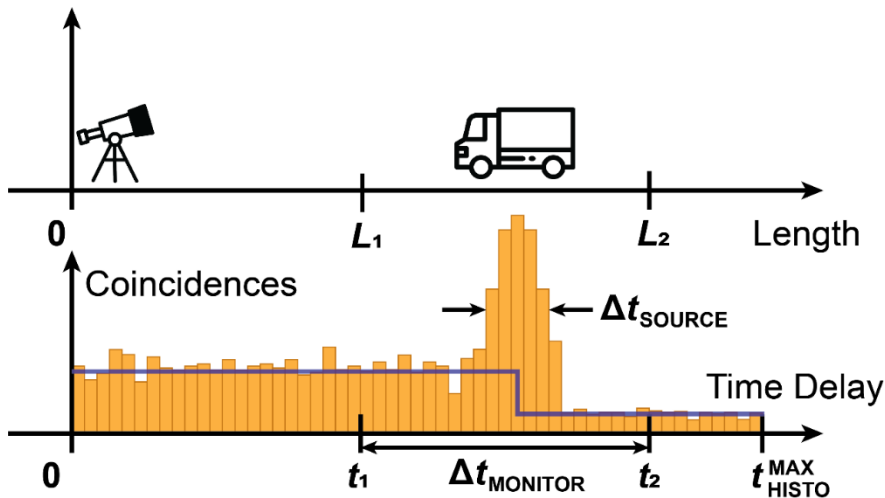
BBO (beta-barium borate)
length 10 mm
pump beam waist 1.0 mm
pump bandwidth 5 nm



Two different-purpose sources have been proposed:

- 1) broadband source for filling the maximum amount of frequency modes (short crystal);
- 2) high-flux source based on a long crystal.

Limitations on the ultimate system performance



- Photon-counting detection limits the max. value of the optical power: time between the adjacent pulses (photons) should be less than $\Delta L/(2c)$ (similar to a lidar).
- Our results demonstrate the detection of targets with reflectance values down to 4% at 6 m distance with 1 s integration time.
- With an optimized source and improved filtering, we expect increase of the ranging distance (up to 100 m), but not the integration time (limitation of the detection method).
- Current sources easily reach the max. available biphoton rate of $\sim 10^6$ Hz.

Range of the monitored distances:

$$\Delta t_{\text{MONITORED}} \equiv \frac{2L}{c} < t_{\text{HISTO}}^{\text{MAX}}$$

Maximal brightness of the source:

$$I_{\text{MAX}} \propto \frac{1}{t_{\text{HISTO}}^{\text{MAX}}}$$

Background suppression coefficient:

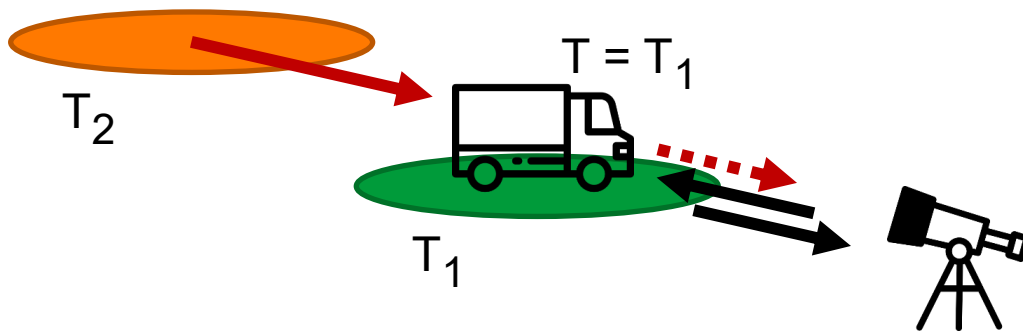
$$\propto b d \frac{t_{\text{HISTO}}^{\text{MAX}}}{\Delta t_{\text{SOURCE}}}$$

$$t_{\text{HISTO}}^{\text{MAX}} (L_1 - L_2 = 100 \text{ m}) > 600 \text{ ns}$$

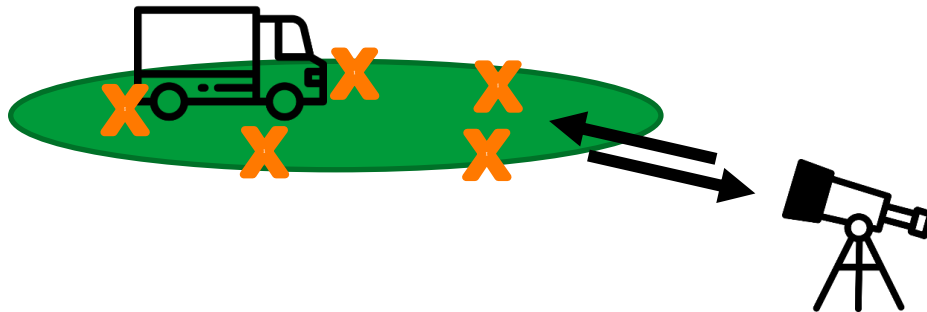
$$I_{\text{MAX}} = \frac{1}{t_{\text{HISTO}}^{\text{MAX}}} < 1 \text{ MHz}$$

Potential applications

In addition to a conventional radar application (send light – detect the reflected light), the following methods can also be used:



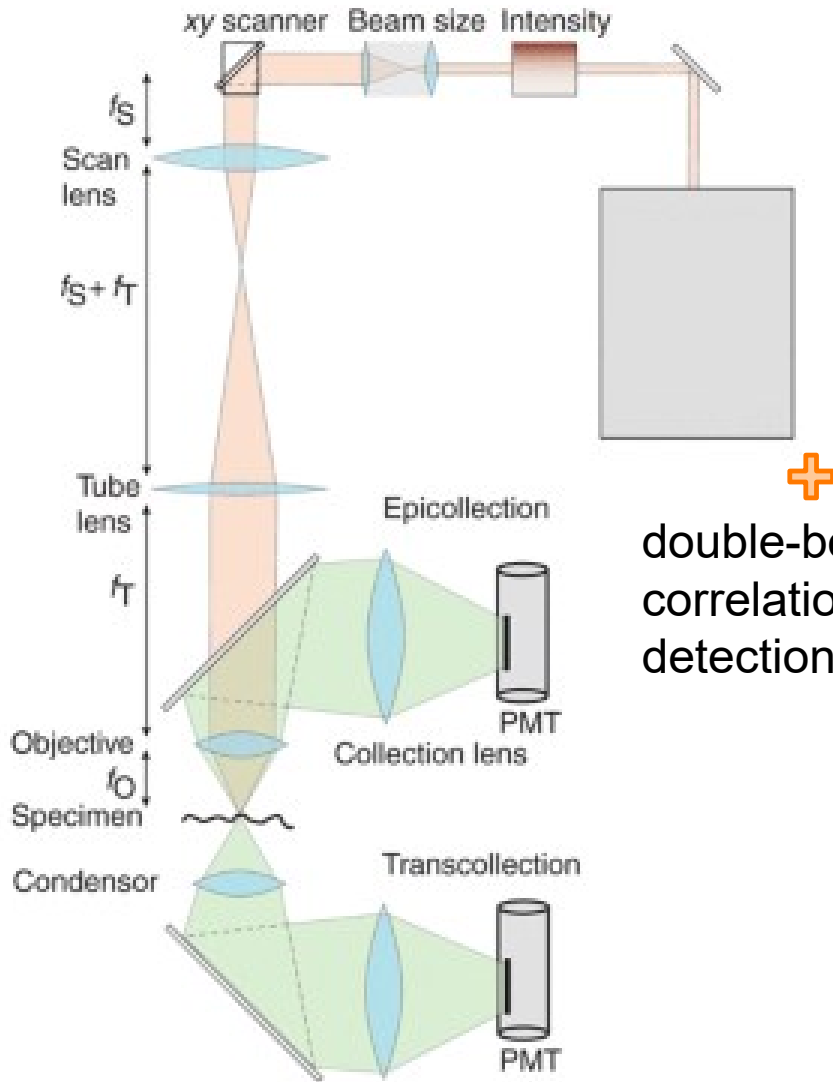
□ Change can be detected in the background radiation (dark red lines, solid and dashed), even when the target has low reflectance thus making the reflectance measurement (black lines) hard.



□ If the background has features providing high reflectance in certain areas (90° retro-reflectors), the change in the reflected signal can be measured.

Working principle: the object (target) changes both how the radar radiation is reflected, and how background radiation is transmitted.

Potential applications



Correlated photons can be used in microscopy applications with light-sensitive specimen: ultraviolet light in biomedical imaging, with the need to reduce the light level.

+

double-beam
correlation-enhanced
detection

Our analytic results help engineering the source of quantum light that would provide the system with the ultimate performance.

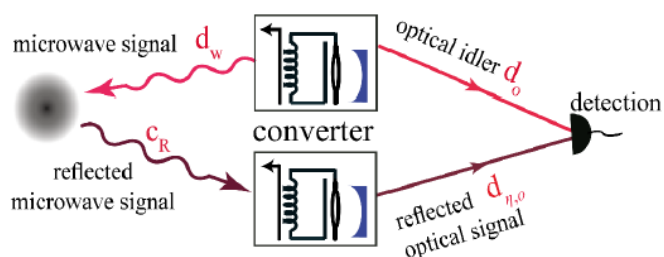
Summary

- ❑ We performed correlation-enhanced target detection with entangled optical photon pairs at 800 nm.
- ❑ Analytical description is developed for the impact of a partially reflecting object on the optical target detection protocol. An undistinguishable ($\mu=1$) jamming object with the reflectance ζ deteriorates the performance of the target detection protocol by a factor of ζ/bd (b – thermal photons per mode, d – number of modes). A quantitative metrics μ of indistinguishability is introduced.
- ❑ We performed the optimization of the photon source for target detection:
 - broadband source (0.25 mm BiBO with 0.1 mm pump beam diameter);
 - high-flux source (10 mm BBO with 1.0 mm pump beam diameter).
- ❑ System performance: detection of targets with reflectance values down to 4% at 6 m distance with 1 s integration time. With an optimized source and improved filtering, expected ranging distance is up to 100 m; integration time – still in the range of a few seconds due to the limitations of the detection method. Maximal available biphoton rate for photon counting is $\sim 10^6$ Hz.
- ❑ Result dissemination in 2023:
 1. Article manuscript submitted to *APL Quantum*.
 2. Conference presentations: CLEO Europe (Munich, Germany); Quantum 2023 (Turin, Italy).
- ❑ The results can be applied to the design of target detection protocols and in developing advanced imaging techniques.

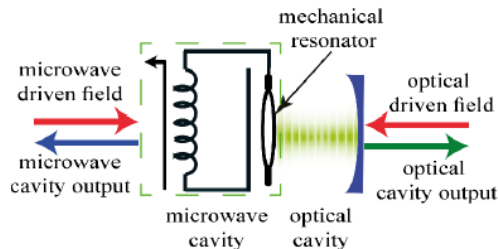


**Thank you for your
attention!**

Correlation-enhanced target detection in the microwave frequency range



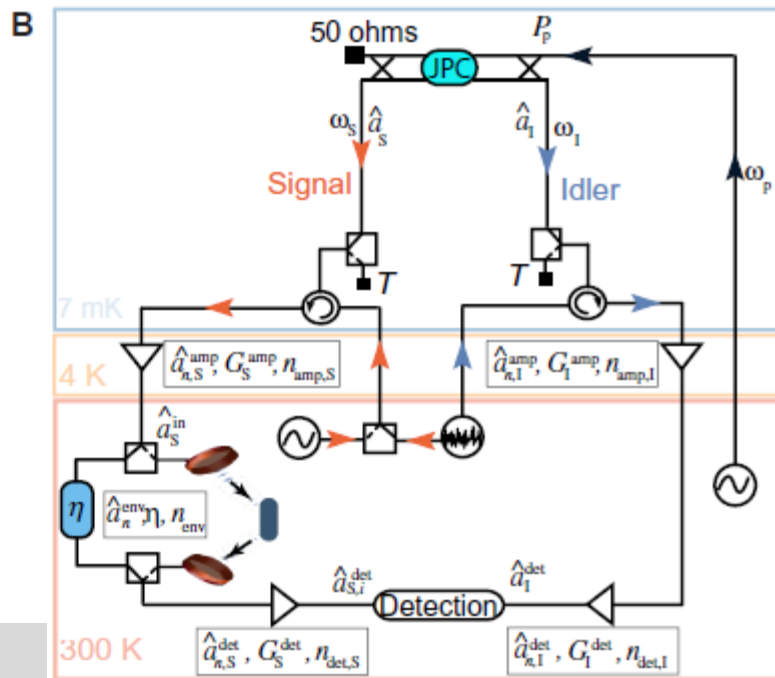
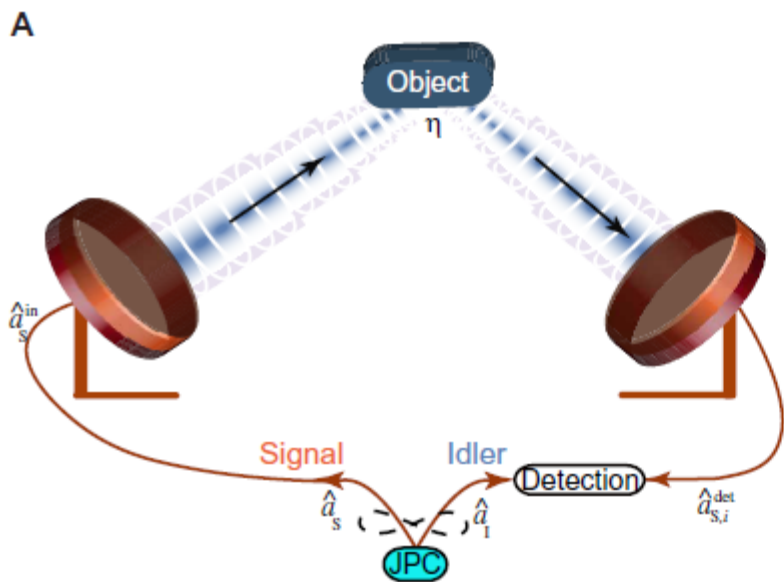
(a) QI radar configuration



(b) EOM converter

[S. Barzanjeh, S. Guha, C. Weedbrook, D. Vitali, J. H. Shapiro, and S. Pirandola, "Microwave quantum illumination" // *Phys. Rev. Lett.* **114**, 080503 (2015).]

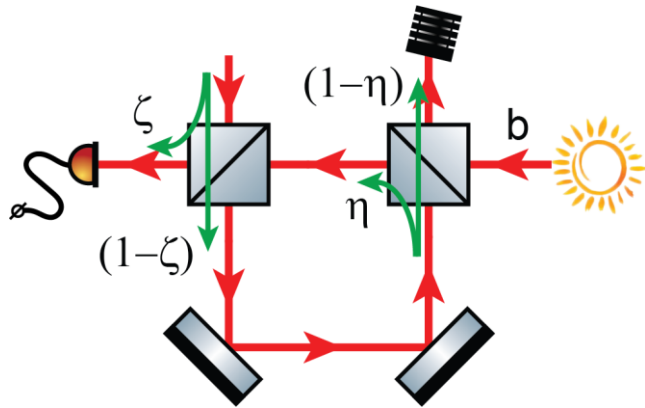
FIG. 4. Schematic for Barzanjeh *et al.*'s microwave quantum illumination [41]. (a) QI radar configuration. (b) Electro-optomechanical (EOM) converter configuration.



[S. Barzanjeh *et al.* // *Sci. Adv.* **6** (19), eabb0451 (2020)]

Protocol details

Double beam interrogation (**DB**) protocol: coincidence counting between the two channels.
 Single beam interrogation (**SB**) protocol: only the photons in the signal channel are used.
 Large number d of radiation modes is assumed. The probabilities ζ and η to detect a photon reflected from the jammer and from the target, correspondingly.
 A weakly reflective jammer ($\zeta \ll 1$) and an even fainter target ($\eta < \zeta$).



Target absent – **SB**:

$$\rho_0 = \zeta \rho_J + (1 - \zeta) (\rho_{TH}) .$$

Target present – **SB** :

$$\rho_1 = \zeta \rho_J + (1 - \zeta) (\eta \rho_T + (1 - \eta) \rho_{TH}) .$$

Thermal background:

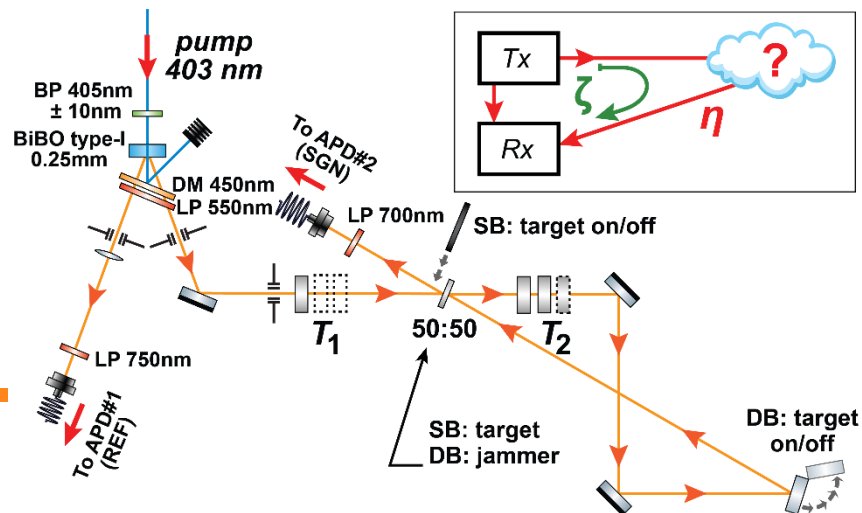
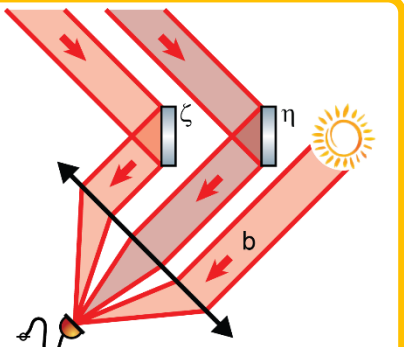
$$\rho_{TH} \approx (1 - bd) |0\rangle_s \langle 0|_s + b \hat{\mathbf{I}}_s \quad \hat{\mathbf{i}}_s \equiv \sum_{k_s=1}^d |1\rangle_{k_s} \langle 1|_{k_s}$$

Alternative multi-mode picture:

$$\rho_1 = \rho_{TH} \otimes$$

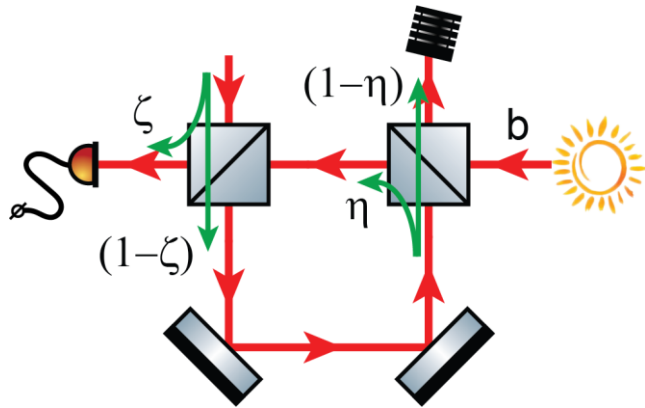
$$\otimes (|0\rangle \langle 0| + \zeta \rho_J) \otimes$$

$$\otimes (|0\rangle \langle 0| + \eta \rho_T) .$$



Protocol details

Double beam interrogation (**DB**) protocol: coincidence counting between the two channels.
 Single beam interrogation (**SB**) protocol: only the photons in the signal channel are used.
 Large number d of radiation modes is assumed. The probabilities ζ and η to detect a photon reflected from the jammer and from the target, correspondingly.
 A weakly reflective jammer ($\zeta \ll 1$) and an even fainter target ($\eta < \zeta$).



Target absent – **DB**:

$$\rho_0 = \zeta \rho_J + (1 - \zeta) (\rho_{TH} \otimes \hat{\mathbf{I}}_i) .$$

Target present – **DB** :

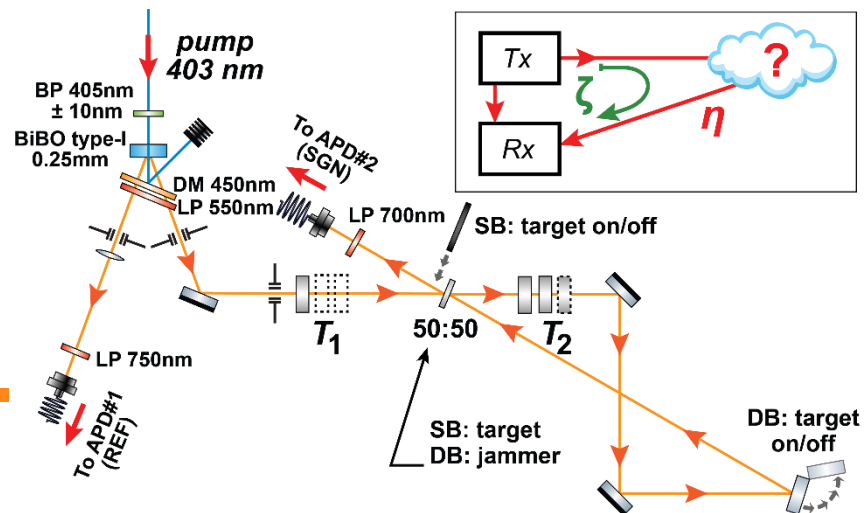
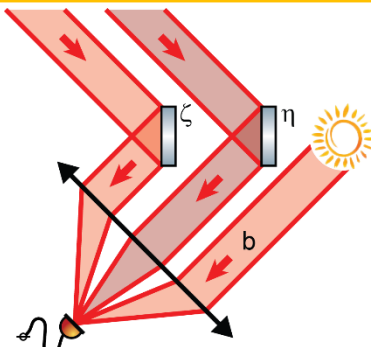
$$\rho_1 = \zeta \rho_J + (1 - \zeta) (\eta \rho_T + (1 - \eta) \rho_{TH} \otimes \hat{\mathbf{I}}_i) .$$

Thermal background:

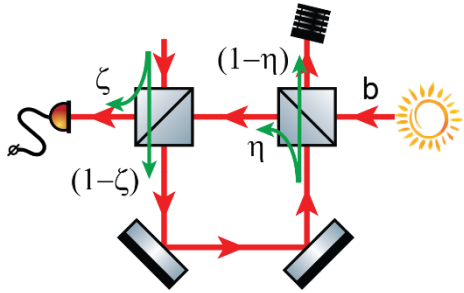
$$\rho_{TH} \approx (1 - bd) |0\rangle_s \langle 0|_s + b \hat{\mathbf{I}}_s \quad \hat{\mathbf{I}}_s \equiv \sum_{k_s=1}^d |1\rangle_{k_s} \langle 1|_{k_s}$$

Alternative multi-mode picture:

$$\rho_1 = \rho_{TH} \otimes (|0\rangle \langle 0| + \zeta \rho_J) \otimes (|0\rangle \langle 0| + \eta \rho_T) .$$



Protocol details



Target absent – **SB**:

$$\rho_0 = \zeta \rho_J + (1 - \zeta) (\rho_{TH}) .$$

Target present:

$$\rho_1 = \zeta \rho_J + (1 - \zeta) (\eta \rho_T + (1 - \eta) \rho_{TH}) .$$

Thermal background:

$$\rho_{TH} \approx (1 - bd) |0\rangle_s \langle 0|_s + b \hat{\mathbf{I}}_s$$

DB: $|\Psi\rangle_{s,i} \approx |0\rangle_s + \frac{A}{\sqrt{d}} \sum_{k=1}^d |1\rangle_{s_k} |1\rangle_{i_k}$

Generated state:

SB: $\rho_{IN}^{SB} = \text{Tr}_i \rho_{IN}^{DB}$

Chernoff bound (N – number of trials):

$$p_{err}^{QCB}(N) = \frac{1}{2} \left(\min_{\alpha \in [0;1]} \text{Tr} \rho_0^{1-\alpha} \rho_1^\alpha \right)^N \equiv \frac{1}{2} \mathcal{F}^N$$

$$N_{min} = \frac{\ln(2p_{err}^{LEV})}{\ln \mathcal{F}} .$$

Protocol details

$$p_{err}^{\text{QCB}}(N) = \frac{1}{2} \left(\min_{\alpha \in [0;1]} \text{Tr} \rho_0^{1-\alpha} \rho_1^\alpha \right)^N \equiv \frac{1}{2} \mathcal{F}^N \quad \begin{aligned} \rho_0 &= \zeta \rho_J + (1 - \zeta) (\rho_{TH}) \\ \rho_1 &= \zeta \rho_J + (1 - \zeta) (\eta \rho_T + (1 - \eta) \rho_{TH}) \end{aligned}$$

Frobenius inner product and Gram-Schmidt orthogonalization:

$$\langle A; B \rangle_F \equiv \text{Tr} AB^\dagger \quad \text{proj}_A B = \frac{\langle B; A \rangle_F}{\langle A; A \rangle_F} A = \frac{\text{Tr} BA^\dagger}{\text{Tr} AA^\dagger} A$$

$$\begin{aligned} \text{Tr} \left(e_1 A_1 + f_1 A_2 + g_1 A_3 \right) \left(e_2 A_1^\dagger + f_2 A_2^\dagger + g_2 A_3^\dagger \right) &= \\ = e_1 e_2 \text{Tr}(A_1 A_1^\dagger) + f_1 f_2 \text{Tr}(A_2 A_2^\dagger) + g_1 g_2 \text{Tr}(A_3 A_3^\dagger) \end{aligned}$$

$$A_1 = |0\rangle \langle 0| ,$$

$$A_2 = \rho_T - \text{proj}_{A_0} \rho_T = \rho_T - \rho_{T00} |0\rangle \langle 0| = \rho'_T ,$$

$$A_3 = \rho_J - \text{proj}_{A_1} \rho_J - \text{proj}_{A_2} \rho_J = \rho'_J - \mu \rho'_T ,$$

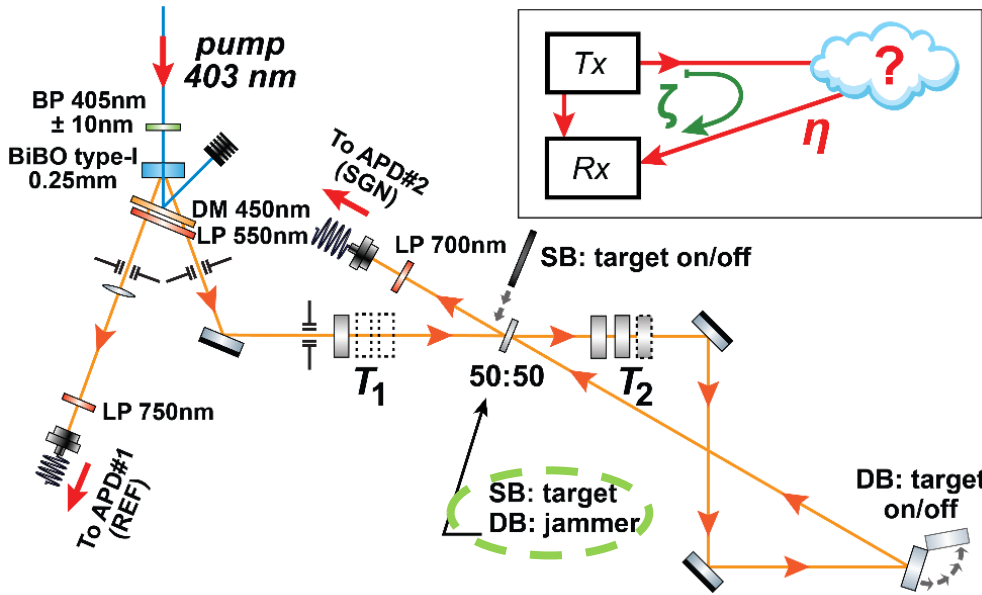
$$A_4 = \hat{\mathbf{I}} - \rho'_J \frac{\text{Tr} \rho'_J - \mu \text{Tr} \rho'_T}{\text{Tr} \rho'^2_J - \mu^2 \text{Tr} \rho'^2_T} - \rho'_T \frac{\frac{\text{Tr} \rho'^2_J}{\text{Tr} \rho'^2_T} \text{Tr} \rho'_T - \mu \text{Tr} \rho'_J}{\text{Tr} \rho'^2_J - \mu^2 \text{Tr} \rho'^2_T} \approx \hat{\mathbf{I}} - \frac{\rho'_J}{1 + \mu} - \frac{\rho'_T}{1 + \mu} .$$

$$A_5 = |0\rangle_s \langle 0|_s \otimes \hat{\mathbf{I}}_i$$

$$A_6 = \hat{\mathbf{I}}_s \otimes |0\rangle_i \langle 0|_i$$

Indistinguishability parameter: $\mu \equiv \frac{\text{Tr} \rho'_J \rho'_T}{\text{Tr} \rho'^2_T} , \quad \mu \in [0; 1]$

Target detection with correlated photons

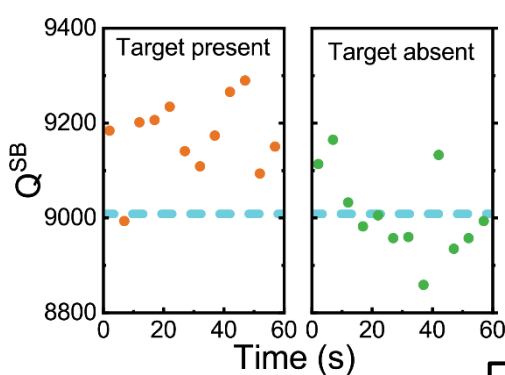


- Single-beam interrogation (SB): only APD#2 is used; APD#1 (REF) is ignored.
- Double-beam interrogation (DB): both APD#1 and APD#2 are used; coincidence detection.

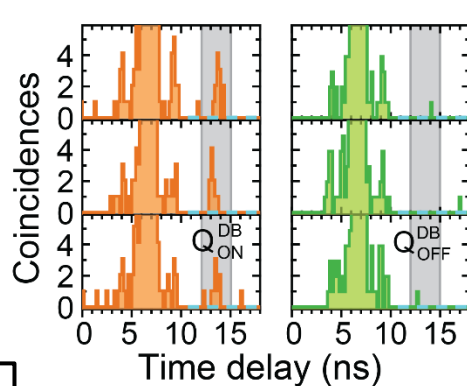
Radiation coming from the jammer (ρ'_J) and from the target (ρ'_T) can be described by an indistinguishability parameter μ :

$$\mu \equiv \frac{\text{Tr} \rho'_J \rho'_T}{\text{Tr} \rho'^2_T}, \quad \mu \in [0; 1]$$

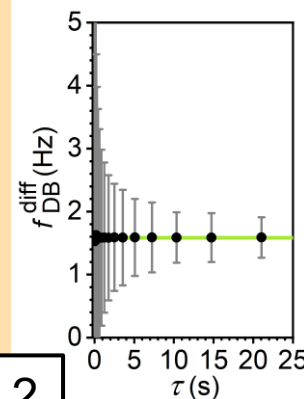
Data processing steps:



1



2



3

